



Lanthanide coordination polymers constructed by a new semirigid bridging salicylamide ligand: Synthesis, structure and luminescence properties



Xue-Qin Song^{*}, Li Wang, Meng-Meng Zhao, Guo-Quan Cheng, Xiao-Run Wang, Yun-Qiao Peng

School of Chemical and Biological Engineering, Lanzhou Jiaotong University, Lanzhou 730070, China

ARTICLE INFO

Article history:

Received 3 July 2013

Received in revised form 21 August 2013

Accepted 21 August 2013

Available online 3 September 2013

Keywords:

Salicylamide ligand

Lanthanide coordination polymer

Crystal structure

Luminescence properties

ABSTRACT

A new semirigid *exo*-bidentate ligand incorporating thenylsalicylamide terminal groups, namely 1,4-bis[[2'-(thenylaminoformyl)phenoxy]methyl]-2,5-bismethylbenzene was synthesized and used as building blocks for constructing lanthanide coordination polymers with luminescent properties. The series of lanthanide nitrate complexes have been characterized by elemental analysis, IR spectroscopy, and X-ray diffraction analysis. All the lanthanide coordination polymers exhibit the same metal-to-ligand molar ratio of 2:3 and the semirigid *exo*-bidentate ligand as a bridging ligand, reacts with lanthanide nitrates forming 1D annular chains $\{[Ln_2(NO_3)_6L_3]_\infty$ ($Ln = Nd$ (**1**), Sm (**2**), Eu (**3**), Tb (**4**)). The samarium, europium and terbium containing compounds exhibit luminescence of the referring trivalent lanthanide ions, giving an orange luminescence for Sm^{III} , a red luminescence for Eu^{III} and a green luminescence for Tb^{III} triggered by an efficient antenna effect of the thenylsalicylamide group.

© 2013 Elsevier B.V. All rights reserved.

1. Introduction

Complexes of lanthanide ions with organic ligands present an astounding class of emissive materials due to peculiarities of their luminescence properties [1]. In such compounds the luminescence of lanthanide ions is explained commonly by the ligand-to-metal energy transfer from the lowest triplet level of the ligands to a resonance level of the lanthanide ion [2]. Generally speaking, to achieve efficient emission, a rare earth ion needs a carefully tailored environment consisting of organic ligands that simultaneously provide a rigid and protective coordination shell for minimizing non-radiative deactivation and ensuring effective population the metal ion excited states through the energy transfer. In recent years, various organic ligands used for constructing luminescent lanthanide coordination polymers have been synthesized [3–5]. Among these numerous ligands, the amide type ligands which have a strong coordination capability towards lanthanide ions and possess strong luminescence properties have been attracting more attention for the preparation of lanthanide complexes [6]. We are interested in the synthesis and characterization of lanthanide complexes with flexible ligands incorporating salicylamide derivatives, and especially in how different types of flexible backbone as well as different

terminal coordination sites can impact the structures as well as the luminescence properties [7].

In a recent paper [6(i)], we described the crystal structure and luminescent properties of lanthanide complexes with a ligand which incorporated 1,4-dimethoxybenzene as a backbone and picolylsalicylamide as pendant arms. The results indicated that the bidentate benzene-bridged space ligand is a useful building block in the construction of luminescent lanthanide coordination polymers with interesting supramolecular properties. In this study, we designed and synthesized a new semirigid *exo*-bidentate ligands incorporating 1,4-dimethylbenzene as backbone and thenylsalicylamide as terminal groups, 1,4-bis[[2'-(thenylaminoformyl)phenoxy]methyl]-2,5-bismethylbenzene (**L**) to extend our systematic research. As a result, a series of novel lanthanide coordination polymers, namely, $[Nd_2(NO_3)_6L_3]_\infty$ (**1**), $[Sm_2(NO_3)_6L_3]_\infty$ (**2**), $[Eu_2(NO_3)_6L_3]_\infty$ (**3**), $[Tb_2(NO_3)_6L_3]_\infty$ (**4**), were synthesized and characterized via single-crystal X-ray diffraction analysis, IR spectra and elemental analysis. The photophysical properties of trivalent Sm , Eu and Tb complexes at room temperature were also investigated in detail. The lowest triplet state energy levels of the ligand was calculated from the phosphorescence spectra of the Gd^{III} complex of the ligand at 77 K. The results presented herein indicated that the new semirigid bridging ligand exhibited a good antennae effect with respect to the Tb^{III} ion due to efficient ligand to metal energy transfer.

^{*} Corresponding author. Tel.: +86 931 4938795; fax: +86 931 4938755.

E-mail addresses: songxq@mail.lzjtu.cn, songxueqin001@163.com (X.-Q. Song).

2. Experimental

2.1. Materials and instrumentation

Thenylamine and 1,4-bimethyl-benzene were obtained from Alfa Aesar Co. Other commercially available chemicals were of analytical grade and were used without further purification. The lanthanide nitrates [8] were prepared according to the literature method.

Carbon, nitrogen and hydrogen analyses were performed using an EL elemental analyzer. Melting points were determined on a Kofler apparatus. Infrared spectra ($4000\text{--}400\text{ cm}^{-1}$) were obtained with KBr discs on a Thermo Mattson FTIR spectrometer. ^1H NMR spectra were recorded in CDCl_3 solution at room temperature on a Bruker 400 instrument operating at a frequency of 400 MHz and referenced to tetramethylsilane (0.00 ppm) as an internal standard. Chemical shift multiplicities are reported as s = singlet, d = doublet, t = triplet and m = multiplet. Fluorescence measurements of the well grinded thick solid samples were made on FLS920 of Edinburgh Instrument equipped with a xenon lamp as the excitation source (front-face mode). Samples were placed between two quartz cover slips and the excitation and emission slit of 0.2 nm were used. The 77 K solution-state phosphorescence spectra of the GdIII complex was recorded with solution samples (a 1:1 ethyl acetate–MeOH (v/v) mixture) loaded in a quartz tube inside a quartz-walled optical Dewar flask filled with liquid nitrogen in the phosphorescence mode on a Hitachi F-4500 spectrophotometer [9]. Quantum yields were determined by an absolute method as described elsewhere [10] using an integrating sphere on FLS920 of Edinburgh Instrument. In this approach, the quantum yield (ϕ_{PL}) is given by: $\phi_{\text{PL}} = \frac{E_i(\lambda) - (1-A)E_0(\lambda)}{L_e(\lambda)A}$, where $A = \frac{L_0(\lambda) - L_i(\lambda)}{L_0(\lambda)}$. According to this notation, $E_i(\lambda)$ and $E_0(\lambda)$ are, respectively, the integrated luminescence as a result of directed excitation of the film and secondary excitation. A is the film absorbance, which is found by measuring the integrated excitation profiles. $L_i(\lambda)$ is the integrated excitation when the film is directly excited and $L_0(\lambda)$ is the integrated excitation when the excitation light first hit the sphere wall. $L_e(\lambda)$ is the integrated excitation profile for an empty sphere. The luminescence decays were recorded using a pumped dye laser (Lambda Physics model FL2002) as the excitation source. The nominal pulse width and the line width of the dye-laser output were 10 ns and 0.18 cm^{-1} , respectively. The emission of the sample was collected by two lenses in a monochromator (WDG30), detected by a photomultiplier and processed by a Boxcar Average (EGG model 162) in line with a microcomputer. Reported quantum yields and luminescence lifetimes are averages of at least three independent determinations. The estimated errors for quantum yields and luminescence lifetimes are 10%.

2.2. Synthesis of the ligand

As shown in Scheme 1, 4-bis[[2'-(thenylaminoformyl)phenoxy]methyl]-2,5-bismethylbenzene (L) was prepared by the following synthetic routes. To a solution of thenylsalicylamide (2.097 g, 9 mmol) in dry acetone (20 mL) was added K_2CO_3 (1.656 g, 12 mmol) and the mixture was stirred and heated for

0.5 h. 1,4-bis(bromomethyl)-2,5-dimethyl-benzene [11] (1.160 g, 4 mmol) in 30 mL of acetone was added dropwise over 30 min, and the resulting solution was stirred and heated to reflux for 10 h. The mixture was cooled to room temperature and distilled water (60 mL) was added to give a crude product. The pure product was obtained using chromatography on silica gel. Chromatography (30–80% ethyl acetate in petroleum ether gradient). Yield: 78%. Mp: 187–188 °C. *Anal. Calc.* for $\text{C}_{34}\text{H}_{32}\text{N}_2\text{O}_4\text{S}_2$: C, 68.43; H, 5.40; N, 4.69; S, 10.75. Found: C, 68.76; H, 5.38; N, 4.68; S, 10.78%. IR (KBr, ν , cm^{-1}): 3377 (s), 2902 (br, m), 1650 (vs), 1598 (m), 1545 (s), 1486 (m), 1451 (m), 1298 (m), 1242 (s), 931 (w), 768 (s). ^1H NMR (CDCl_3 , 400 MHz, ppm): δ 2.18 (s, 6H, $-\text{CH}_3$), 4.68 (d, 4H, $-\text{CH}_2-$), 5.11 (s, 4H, $-\text{CH}_2-$), 6.73 (d, 2H ArH), 6.80 (m, 2H, ArH), 7.07–7.16 (m, 8H, ArH), 7.46–7.50 (m, 2H, ArH), 8.17 (s, 2H, $-\text{NH}-$), 8.29 (dd, 2H, ArH), ESI-MS: m/z 597.7 ($\text{M}+\text{H}^+$).

2.3. Synthesis of the lanthanide nitrate complex

$[\text{Nd}_2(\text{NO}_3)_6\text{L}_3]_\infty$ (**1**): 59.8 mg (0.1 mmol) L and 43.8 mg (0.1 mmol) $\text{Nd}(\text{NO}_3)_3 \cdot 6\text{H}_2\text{O}$ were dissolved in a hot methanol + ethyl acetate (v/v = 1:10) solution to make a concentrated solution. Then the flask was cooled, and the mixture was filtered into a sealed 10–20 mL glass vial for crystallization at room temperature. After about 2 weeks, pale purple single crystals of 1 suitable for crystal analysis were obtained. (Yield: 84.5 mg, 69% based on $\text{Nd}(\text{NO}_3)_3 \cdot 6\text{H}_2\text{O}$). *Anal. Calc.*: C, 49.99; H, 3.95; N, 6.86; S, 7.85. Found: C, 49.78; H, 3.95; N, 6.84; S, 7.81%. IR (KBr, ν cm^{-1}): 3421 (m), 2924 (m), 2850 (w), 1615 (s), 1564 (m), 1478 (s), 1301 (s), 1235 (m), 1032 (m), 988 (m), 816 (w), 756 (m).

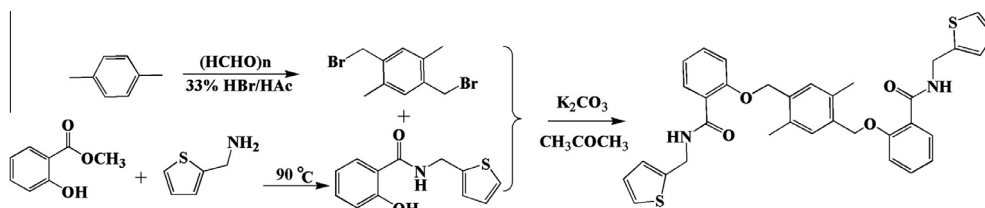
$[\text{Sm}_2(\text{NO}_3)_6\text{L}_3]_\infty$ (**2**): The procedure was the same as that for 1 using $\text{Sm}(\text{NO}_3)_3 \cdot 6\text{H}_2\text{O}$. Colorless single crystals of 2 were formed after 2 weeks. (Yield: 80 mg, 65% based on $\text{Sm}(\text{NO}_3)_3 \cdot 6\text{H}_2\text{O}$). *Anal. Calc.*: C, 49.74; H, 3.93; N, 6.82; S, 7.81. Found: C, 49.98; H, 3.94; N, 6.78; S, 7.84%. IR (KBr, ν): 3426 (m), 2930 (m), 2852 (w), 1615 (s), 1560 (m), 1480 (s), 1302 (s), 1232 (m), 1032 (m), 988 (m), 818 (w), 755 (m).

$[\text{Eu}_2(\text{NO}_3)_6\text{L}_3]_\infty$ (**3**): The procedure was the same as that for 1 using $\text{Eu}(\text{NO}_3)_3 \cdot 6\text{H}_2\text{O}$. Colorless single crystals of 2 were formed after 2 weeks. (Yield: 67.8 mg, 55% based on $\text{Eu}(\text{NO}_3)_3 \cdot 6\text{H}_2\text{O}$). *Anal. Calc.*: C, 49.67; H, 3.92; N, 6.82; S, 7.80. Found: C, 49.48; H, 3.94; N, 6.80; S, 7.83%. IR (KBr, ν): 3421 (m), 2928 (m), 2848 (w), 1616 (s), 1558 (m), 1482 (s), 1300 (s), 1232 (m), 1032 (m), 988 (m), 816 (w), 756 (m).

$[\text{Tb}_2(\text{NO}_3)_6\text{L}_3]_\infty$ (**4**): The procedure was the same as that for 1 using $\text{Tb}(\text{NO}_3)_3 \cdot 6\text{H}_2\text{O}$. Colorless single crystals of 2 were formed after 2 weeks. (Yield: 74.4 mg, 60% based on $\text{Tb}(\text{NO}_3)_3 \cdot 6\text{H}_2\text{O}$). *Anal. Calc.*: C, 49.40; H, 3.90; N, 6.78; S, 7.76. Found: C, 49.28; H, 3.91; N, 6.80; S, 7.75%. IR (KBr, ν): 3424 (m), 2930 (m), 2852 (w), 1616 (s), 1558 (m), 1478 (s), 1300 (s), 1230 (m), 1032 (m), 988 (m), 818 (w), 756 (m).

2.4. X-ray single-crystal diffraction analysis

Crystals of complexes **1–4** with approximate dimensions of $0.21 \times 0.17 \times 0.12\text{ mm}^3$, $0.15 \times 0.12 \times 0.08\text{ mm}^3$, $0.14 \times 0.11 \times 0.08\text{ mm}^3$, $0.15 \times 0.12 \times 0.08\text{ mm}^3$, suitable for



Scheme 1. The synthetic route of the ligand L.

X-ray diffraction, were obtained in good yield by slow evaporation of the mixed solvent (ethyl acetate/methanol = 10:1, v/v) in air over 2 weeks. The crystals belonged to the triclinic space group $P\bar{1}$. The data were collected at 296 K using a Bruker Smart APEX II CCD diffractometer equipped with graphite-monochromatized Mo Cu $K\alpha$ radiation ($\lambda = 0.71073$ Å). The structure was solved by direct methods and all non-hydrogen atoms were subjected to anisotropic refinement by full-matrix leastsquares methods on F^2 data using the software package SHELXS-97 [12]. Hydrogen atoms were placed at calculated positions and refined isotropically. Crystallographic data as well as details of data collection and refinement for these complexes are summarized in Table 1, and important bond lengths are listed in Table 2.

3. Results and discussion

3.1. Synthesis

The ligand L was prepared by the ether base coupling of 1,4-bis(bromomethyl)-2,5-dimethyl-benzene and thenylsalicylamide in a 1:2.25 ratio in dry acetone in the presence of an excess of anhydrous K_2CO_3 . One of the important issues in determining the framework structures is the geometry of the organic ligands. In our study, the terminal coordinating donors are separated by the 1,4-dimethylbenzene backbone at the para position, and two salicylamide arms are rotationally free and are thus capable of adjusting to match the metal coordination preference well. The new ligand gave satisfactory 1H NMR, IR spectra, mass spectrometry, and elemental analyses. The complexes are soluble in DMF, DMSO, methanol and ethanol, slightly soluble in ethyl acetate, acetonitrile and acetone, but insoluble in $CHCl_3$ and ether. X-ray quality crystals of the complexes were obtained after several weeks by slow evaporation of ethyl acetate solution containing ligand L and corresponding LnIII ions. The characteristic band of the carbonyl group of free ligand L in IR spectra (Fig. S1) is shown at 1650 cm^{-1} . The absence of the band round 1650 cm^{-1} , which is instead of a new band at ca. 1616 cm^{-1} of the complexes (Figs. S2–S5) compared to free ligand, indicates the complete coordination of the ligand. Weak absorptions observed in the range of $2924\text{--}2930\text{ cm}^{-1}$ can

be attributed to the $\nu(CH_2)$ of the ligand. The ν_3 of the free nitrate group (1380 cm^{-1}) disappears in the spectra of the complexes, implying that three nitrate groups are all in coordination sphere. The bands assigned to the coordinated nitrates were observed as two group bands at about $1482\text{ cm}^{-1}(\nu_1)$ and $1300\text{ cm}^{-1}(\nu_4)$ for the complexes and the differences between the strongest absorption band ν_1 and ν_4 of nitrate group lie in ca 182 cm^{-1} , indicating that coordinated nitrate groups in the complexes are bidentate ligands [13] which is in agreement with the crystal analysis as follows.

3.2. Crystal structure descriptions

Block crystals of **1–4** were obtained by reaction of $Ln(NO_3)_3 \cdot 6H_2O$ and L in a 3:2 M ratio in ethyl acetate/methanol solution. X-ray crystal structure analyses reveal that **1–4** are isostructural and crystallize in the triclinic space group $P\bar{1}$, showing a slight contraction of the Ln coordination sphere as expected. Thus, only **3** is selected for investigation here in detail as the representative example. In complex **3**, the asymmetric unit consists of one and half ligands and one crystallographically independent EuIII ion. As depicted in Fig. 1a, the EuIII center is nine-coordinated and is surrounded by three carbonyl oxygen atoms coming from three different ligands (O1, O3, O5) and six nitrate oxygen atoms (O7, O8, O10, O11, O13, O14). Each EuIII ion adopts a distorted monocapped square antiprismatic geometry and the square antiprism is described by three O atoms from ligand (O1, O3 and O5) and five O atoms from nitrate anions (O7, O8, O10, O13 and O14) while the vertex occupied by the O atom from one nitrate anion (O11) (Fig. 1b). The Eu–O (nitrate) bond lengths span the range of $2.425(9)\text{--}2.542(9)$ Å, however, the Eu–O(carbonyl) bond lengths vary obviously from $2.329(9)$ to $2.401(9)$ Å, both of which fall into normal ranges. As seen from Fig. 2a, each metal center forms a “Y-joint” connecting unit for the bidentate bridging ligand, and these units are arranged to produce a 1D edge-sharing annular chain. The geometry of the salicylamide groups around the europium atom slightly deviates from ideal values ($O5\text{--}Eu1\text{--}O1 = 144.5(3)^\circ$, $O5\text{--}Eu1\text{--}O3 = 74.2(3)^\circ$, $O1\text{--}Eu1\text{--}O3 = 138.4(3)^\circ$) and the ligand adopt a energy favorable trans configuration in complex **3**. The

Table 1
Crystal data and structure refinement parameters for **1–4**.

| | 1 | 2 | 3 | 4 |
|--|---|--|--|--|
| Empirical formula | $C_{51}H_{46}N_6NdO_{15}S_3$ | $C_{50}H_{44}N_6O_{15}S_3Sm$ | $C_{51}H_{47}EuN_6O_{15}S_3$ | $C_{51}H_{45}N_6O_{15}S_3Tb$ |
| T (K) | 296(2) | 296(2) | 296(2) | 293(2) |
| M | 1224.37 | 1215.48 | 1232.13 | 1237.07 |
| Crystal system, space group | triclinic, $P\bar{1}$ | triclinic, $P\bar{1}$ | triclinic, $P\bar{1}$ | triclinic, $P\bar{1}$ |
| a (Å) | 11.653(4) | 11.658(3) | 11.6750(12) | 11.6821(18) |
| b (Å) | 13.474(4) | 13.425(3) | 13.4290(14) | 13.382(2) |
| c (Å) | 17.566(6) | 17.524(4) | 17.5070(18) | 17.527(3) |
| A ($^\circ$) | 89.293(7) | 83.115(4) | 82.898(5) | 82.875(3) |
| B ($^\circ$) | 79.055(7) | 78.935(4) | 78.727(2) | 78.515(3) |
| γ ($^\circ$) | 86.211(6) | 86.523(4) | 86.532(5) | 86.809(4) |
| V (Å 3) | 2686.7(15) | 2670.2(10) | 2669.3(5) | 2663.0(7) |
| Z | 2 | 2 | 2 | 2 |
| D_{calc} (kg m $^{-3}$) | 1.512 | 1.510 | 1.533 | 1.543 |
| μ (mm $^{-1}$) | 1.155 | 1.289 | 1.356 | 1.518 |
| $F(000)$ | 1244 | 1230 | 1252 | 1252 |
| θ Range for data collection/deg | 1.78–25.15 | 1.78–28.44 | 1.53–25.00 | 1.83–25.15 |
| Index ranges | $-13 \leq h \leq 7$ $-16 \leq k \leq 16$ $-21 \leq l \leq 21$ | $-12 \leq h \leq 15$ $-17 \leq k \leq 17$ $-23 \leq l \leq 21$ | $-13 \leq h \leq 13$ $-15 \leq k \leq 13$ $-20 \leq l \leq 19$ | $-11 \leq h \leq 13$ $-15 \leq k \leq 13$ $-20 \leq l \leq 20$ |
| Independent reflections (R_{int}) | 0.0622 | 0.0403 | 0.0953 | 0.0341 |
| Reflections collected/unique | 15017/9517 | 18321/12862 | 14500/9380 | 14714/9510 |
| Data/restraints/parameters | 9517/725/58 | 12862/689/0 | 9380/707/0 | 9510/688/37 |
| Goodness-of-fit on F^2 | 1.011 | 0.980 | 0.871 | 1.008 |
| Final R indices [$I > 2\sigma(I)$] | $R_1 = 0.0806$, $wR_1 = 0.1981$ | $R_1 = 0.0707$, $wR_1 = 0.1860$ | $R_1 = 0.0839$, $wR_1 = 0.1945$ | $R_1 = 0.0588$, $wR_1 = 0.1526$ |
| R indices (all data) | $R_2 = 0.1317$, $wR_2 = 0.2565$ | $R_2 = 0.1203$, $wR_2 = 0.2269$ | $R_2 = 0.1727$, $wR_2 = 0.2461$ | $R_2 = 0.089$, $wR_2 = 0.1892$ |

Table 2
Representative bond lengths (Å) for complexes 1–4.

| | | | | | | | | | |
|---------|----------|---------|----------|---------|----------|---------|----------|--------|----------|
| Nd1–O1 | 2.434(6) | Nd1–O2 | 2.380(7) | Nd1–O3 | 2.396(7) | Nd1–O1 | 2.535(8) | Nd1–O5 | 2.488(7) |
| Nd1–O7 | 2.558(9) | Nd1–O8 | 2.434(6) | Nd1–O10 | 2.493(7) | Nd1–O11 | 2.585(8) | | |
| Sm1–O1 | 2.348(5) | Sm1–O3 | 2.397(5) | Sm1–O5 | 2.358(5) | Sm1–O7 | 2.451(5) | Sm1–O8 | 2.517(6) |
| Sm1–O10 | 2.518(6) | Sm1–O11 | 2.433(5) | Sm1–O13 | 2.494(6) | Sm1–O14 | 2.561(5) | | |
| Eu1–O5 | 2.329(9) | Eu1–O1 | 2.336(9) | Eu1–O3 | 2.401(9) | Eu1–O10 | 2.425(9) | Eu1–O8 | 2.429(9) |
| Eu1–O14 | 2.497(9) | Eu1–O11 | 2.519(9) | Eu1–O7 | 2.524(9) | Eu1–O13 | 2.542(9) | | |
| Tb1–O1 | 2.309(5) | Tb1–O2 | 2.322(6) | Tb1–O3 | 2.455(6) | Tb1–O4 | 2.535(7) | Tb1–O6 | 2.404(7) |
| Tb1–O7 | 2.479(7) | Tb1–O9 | 2.497(7) | Tb1–O10 | 2.403(6) | Tb1–O15 | 2.365(6) | | |

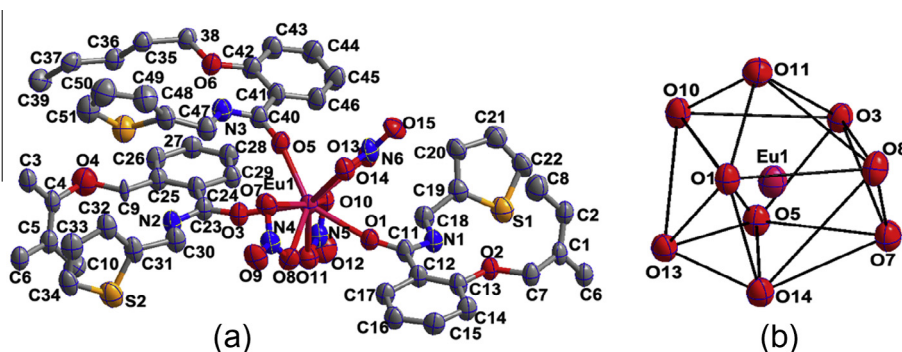


Fig. 1. (a) Local coordination environment of the EuIII ions in **3** with thermal ellipsoids at 30% probability. Hydrogen atoms are omitted for clarity. Symmetry codes: $i = x, y, z$; $ii = -x, -y, -z$. (b) Coordination polyhedron of EuIII ions in **3**.

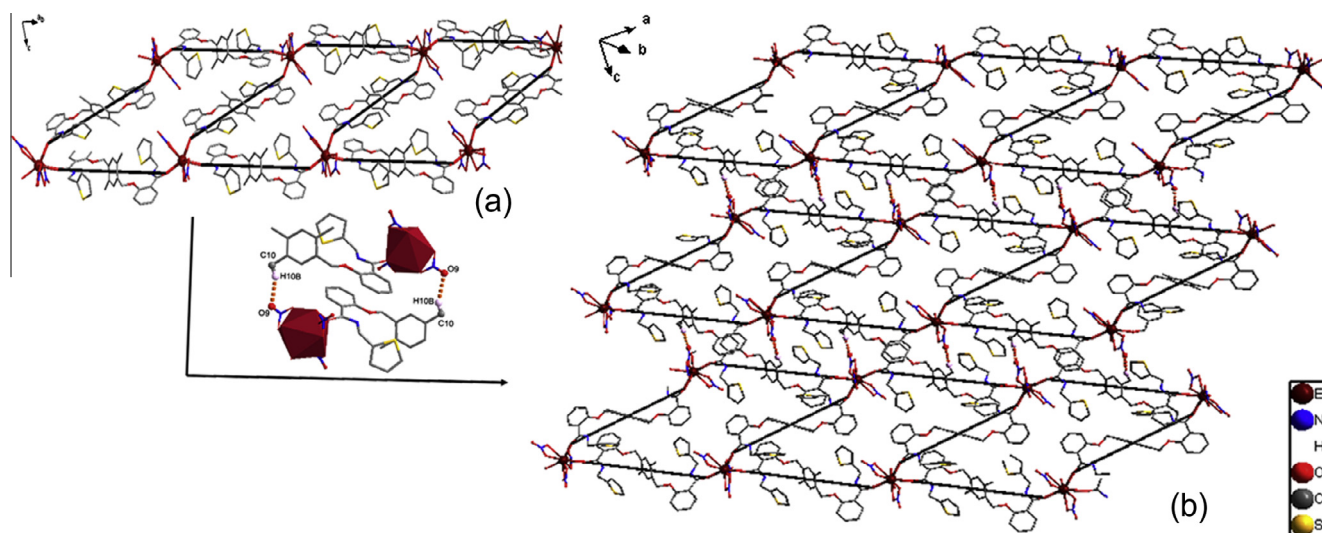


Fig. 2. (a) The 1D edge-sharing annular chain **3**. (b) 2D supramolecular network constructed by C–H...O hydrogen bonding as well as π ... π stacking which are indicated with dashed yellow lines. (hydrogen atoms, except those forming hydrogen bonds, are omitted for clarity). (For interpretation of the references to color in this figure legend, the reader is referred to the web version of this article.)

simplest cyclic motif of the annular chain is a large quadrangled 64-membered ring consisting of four L linkers alternately bridging four $\text{Eu}(\text{NO}_3)_3$ moieties and the metal–metal distances in each quadrangle ring are slightly different: $\text{Eu1}\cdots\text{Eu1} = 18.320(6)$ Å, $\text{Eu1}\cdots\text{Eu1} = 7.982(4)$ Å. Upon careful investigation of the structure, it can be seen that the 1D annular chains are held together to a puckered two-dimensional (2D) supramolecular network via C–H...O hydrogen bonding [14] between nitrate O atoms and methyl carbon atoms (Fig. 2b). The $\text{C10}\cdots\text{O9}$ distance (3.456 Å), $\text{C10}\text{--}\text{H10B}\cdots\text{O9}$ angle (156.38) are all within the ranges of those reported C–H...O hydrogen bonds [15]. In addition, a interchain offset π ... π stacking interaction between the ring $\text{C12}\text{--}\text{C13}\text{--}\text{C14}\text{--}\text{C15}\text{--}\text{C16}\text{--}\text{C17}$ with the centroid–centroid distance of 4.831 Å (Fig. 2b) and the plane–plane distance of 3.766 Å further stabilize the 2D supramolecular network. The general trend of decreasing

$\text{Ln}\text{--}\text{O}$ distance in the series $\text{Nd}^{3+} > \text{Sm}^{3+} > \text{Eu}^{3+} > \text{Tb}^{3+}$ reflects a decrease in ionic radii.

3.3. Luminescence properties of ligands and their complexes in the solid state

Upon UV irradiation, the free ligand emits at ca. 384 nm which is very similar to that of salicylamide derivatives reported before [6]. However, upon complexation with trivalent lanthanide this emission is replaced by the typical luminescent color arising from SmIII, EuIII and TbIII cations. The luminescence characteristics of lanthanide complexes in solid state were measured at room temperature under identical experimental conditions, and the luminescence data in solid state are listed in Table 3.

The excitation spectrum of EuIII complex (Fig. 3) shows evidence of direct metal-centered absorption bands, with sharp peaks at 396 nm which we assign to the ${}^7F_0 \rightarrow {}^5L_6$ transitions [16]. Also present in the spectrum is a weak broad absorption overlap with a peak maximum at ca. 318 and 351 nm, which originates from the intraligand $\pi-\pi^*$ transition of the coordinated ligand on the basis of previous reports which indicates that the EuIII luminescence is not efficiently sensitized by the ligand which is also similar to the reported previously [6,7]. The emission spectrum of EuIII complex (Fig. 4) at room temperature upon excitation at 396 nm exhibits the characteristic transition of EuIII ion. They are originated from the ${}^5D_0 \rightarrow {}^7F_J$ ($J = 0, 1, 2, 3$ and 4) transitions, i.e., 579 nm (${}^5D_0 \rightarrow {}^7F_0$), 592 and 594 nm (${}^5D_0 \rightarrow {}^7F_1$), 617 nm (${}^5D_0 \rightarrow {}^7F_2$), 548 nm (${}^5D_0 \rightarrow {}^7F_3$) and 686, 695, 697 nm (${}^5D_0 \rightarrow {}^7F_4$). The most intense transition is ${}^5D_0 \rightarrow {}^7F_2$ (electric dipole) which is much stronger than that of the ${}^5D_0 \rightarrow {}^7F_1$ transition (magnetic dipole) implies red emission light of EuIII complex. Additionally, because the ${}^5D_0 \rightarrow {}^7F_0$ transition is strictly forbidden in a field of symmetry and is only allowed for C_s , C_n , and C_{nv} site symmetries according to the ED selection rule [17], the symmetry-forbidden emission ${}^5D_0 \rightarrow {}^7F_0$ found at about 579 nm reveals that EuIII ions occupy sites with low symmetry and without an inversion center, which is in good agreement with the single-crystal X-ray analysis.

The photoluminescence properties of TbIII complex were also investigated in detail. From the excitation spectrum (Fig. 5), the biggest broad band with the maximum value at 320 nm is attributed to the overlapping of the $\pi-\pi^*$ electron transition of the ligand and the spin allowed $4f^8 \rightarrow 4f^75d^1$ (${}^7F_6 \rightarrow {}^7D$) transition with higher energy ($\Delta S = 0$), and the spin-forbidden $4f^8 \rightarrow 4f^75d^1$ (${}^7F_6 \rightarrow {}^9D$) transition with lower energy ($\Delta S = 1$) of the TbIII ions. The characteristic f \rightarrow f transition lines within the $4f^8$ configuration of the TbIII ions are in the longer wavelength region (330–500 nm), assigned as the transitions from the 7F_6 ground state to the different excited states of the TbIII ions, that is, 345 nm (5G_2), 356 nm (5D_2), 363 nm (${}^5L_{10}$), 375 nm (5G_6), 381 nm (5D_3) and 490 nm (5D_4). Excitation of TbIII complex of L at 320 nm displays intense green luminescence and exhibits the characteristic transitions of TbIII ion. As shown in Fig. 6, the peaks at 491, 545, 588, 623 and 646 nm are attributed to the ${}^5D_4 \rightarrow {}^7F_6$, ${}^5D_4 \rightarrow {}^7F_5$, ${}^5D_4 \rightarrow {}^7F_4$, ${}^5D_4 \rightarrow {}^7F_3$ and ${}^5D_4 \rightarrow {}^7F_2$ transitions, respectively. Among these characteristic emission transitions, the strongest one is located at 545 nm, in the green region.

In addition to steady-state measurements, the luminescence lifetimes of the Eu(5D_0) and Tb(5D_4) excited states and quantum yield determinations for Eu, Tb complex of L were determined with the results also summarized in Table 3. The relatively long luminescence lifetimes and larger quantum yield values are an

Table 3
Luminescence data for SmIII, EuIII and TbIII complexes.

| | λ_{ex} (nm) | λ_{em} (nm) | Assignment | τ^a | Φ (%) ^a |
|--|---------------------|---------------------|---------------------------------------|------------|-------------------------|
| SmL _{3/2} (NO ₃) ₃ | 320 | 564 | ${}^4G_{5/2} \rightarrow {}^6H_{5/2}$ | 12 μ s | – |
| | | 597 | ${}^4G_{5/2} \rightarrow {}^6H_{7/2}$ | | |
| EuL _{3/2} (NO ₃) ₃ | 396 | 579 | ${}^5D_0 \rightarrow {}^7F_0$ | 1.067 ms | 32.7 |
| | | 592, 594 | ${}^5D_0 \rightarrow {}^7F_1$ | | |
| | | 617 | ${}^5D_0 \rightarrow {}^7F_2$ | | |
| | | 686, 695, 697 | ${}^5D_0 \rightarrow {}^7F_4$ | | |
| | | | ${}^5D_0 \rightarrow {}^7F_3$ | | |
| TbL _{3/2} (NO ₃) ₃ | 320 | 491 | ${}^5D_4 \rightarrow {}^7F_6$ | 1.344 ms | 56.1 |
| | | 545 | ${}^5D_4 \rightarrow {}^7F_5$ | | |
| | | 588 | ${}^5D_4 \rightarrow {}^7F_4$ | | |
| | | 623 | ${}^5D_4 \rightarrow {}^7F_3$ | | |
| | | 646 | ${}^5D_4 \rightarrow {}^7F_2$ | | |
| | | | ${}^5D_4 \rightarrow {}^7F_2$ | | |

^a Luminescence lifetimes and quantum yield values are reported here with an error of $\pm 10\%$.

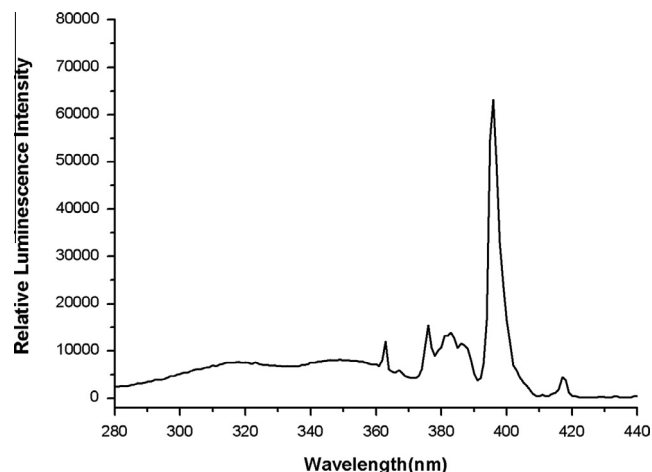


Fig. 3. Room-temperature excitation spectra for europium complex of ligand L with emission monitored at approximately 617 nm in the solid state.

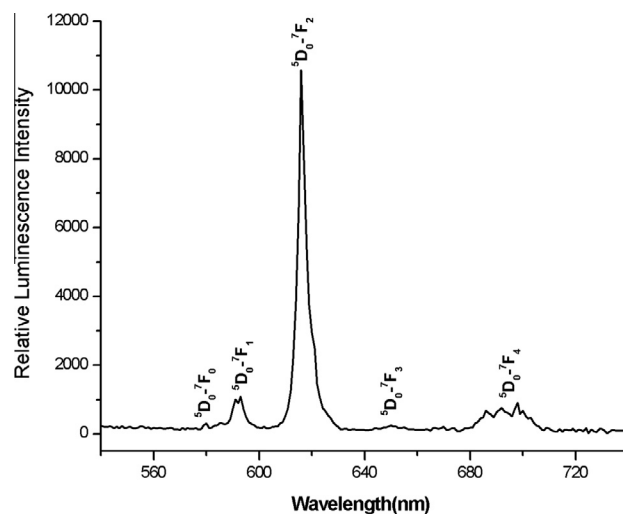


Fig. 4. Room-temperature emission spectra for europium complex of ligand L ($\lambda_{ex} = 396$ nm) in the solid state.

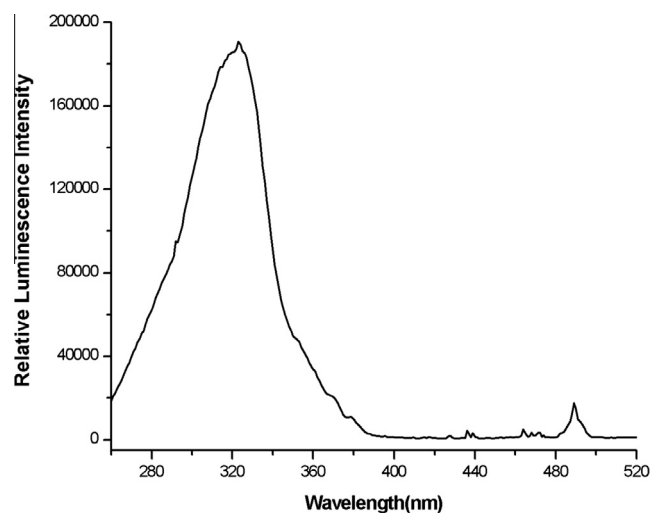


Fig. 5. Room-temperature excitation spectra for terbium complex of ligand L with emission monitored at approximately 545 nm in the solid state.

indication that the bridging ligand provides a significant level of protection from nonradiative deactivation of lanthanide cations by the solvent molecules. However, the longer lifetime and the larger quantum yield of TbIII than that of EuIII is most likely due to the insufficient inter-system crossing (ISC) of EuIII complexes, as further supported by the energy transfer discussed below.

Because the lowest excited state, ${}^6P_{7/2}$ ($E({}^6P_{7/2}) = 32000\text{ cm}^{-1}$) of GdIII is too high to accept energy from the ligand, the data obtained from the phosphorescence spectra actually reveal the triplet energy level of ligand in lanthanide complexes. To demonstrate the energy transfer process, the phosphorescence spectrum of GdIII complex of L (Fig. 7) was measured for the triplet energy-level data. In general, the sensitization pathway in luminescent europium complexes consists of excitation of the ligands into their excited singlet states, subsequent intersystem crossing of the ligands to their triplet states and energy transfer from the triplet state to the 5D_J manifold of the EuIII ions, followed by internal conversion to the emitting 5D_0 state. Finally, the EuIII ion emits when a transition to the ground state occurs [18]. Consequently, most europium complexes give rise to typical emission bands at ca 581, 593, 614, 654 and 702 nm, corresponding to the deactivation of the 5D_0 excited state to the 7F_J ground states ($J=0-4$). In a similar way, the 4f electrons of the TbIII ion are excited to the 5D_J ion manifold from the ground state. Finally, the TbIII ion emits when the 4f electrons undergo a transition from the excited state of 5D_4 to the 7F_J ground states ($J=6-3$). Latva's empirical rule [19] states that an optimal ligand-to-metal energy transfer process for LnIII needs $\Delta E = {}^3\pi\pi^* - {}^5D_J$ [2500–4000 cm^{-1} for EuIII and 2500–4500 cm^{-1} for TbIII]. From the phosphorescence spectra (Fig. 7), the triplet energy level (${}^3\pi\pi^*$) of GdIII complex, which corresponds to its lower wavelength emission edge, is 25125 cm^{-1} (398 nm). The triplet energy level of the salicylamide ligand (25125 cm^{-1}) is higher than the 5D_0 level of EuIII (17500 cm^{-1}) and the 5D_4 level of TbIII (20400 cm^{-1}). This therefore supports the observation of stronger sensitization of the terbium complexes than the europium complexes because of the smaller overlap between the ligand triplet and europium ion excited states.

In order to demonstrate the capability of antenna-modified ligands as sensitizers for lanthanides other than the commonly used europium and terbium, we extended our work to SmIII complex. The excitation spectra registered at the maximum of the SmIII emissions are in line with previous observations for the terbium complex. Upon excitation at $\lambda_{\text{ex}} = 320\text{ nm}$, typical emission spectra

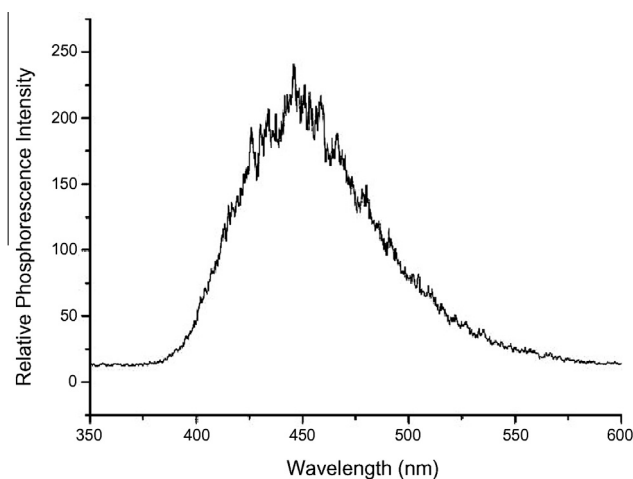


Fig. 7. Phosphorescence spectra of GdIII complex of ligand L in methanol-ethyl acetate solution at 77 K.

of SmIII was detected (Fig. 8). The emission lines at 564 and 597 nm are assigned to ${}^4G_{5/2} \rightarrow {}^6H_J$ transitions, with $J=5/2$ and $7/2$, respectively. The relatively strong peak is the ${}^4G_{5/2} \rightarrow {}^6H_{7/2}$ transition at 597 nm. Generally, the luminescence spectra of SmIII were quite weak. Quantum yields are expected to be very small and their measurements were therefore omitted. Lifetime measurements for the Sm complexes are found to be 12 μs , based on a single-exponential fit of the data. The higher sensitivity of samarium derived luminescence, in comparison with europium or terbium luminescence, can be explained by the energy gap between the excited luminescent states and the highest J levels of the ground states of these lanthanides. This energy gap is about 7500 cm^{-1} for SmIII, that is, considerably smaller than that for EuIII and TbIII ions with values around 12300 cm^{-1} and 14800 cm^{-1} , respectively [20]. In the case of samarium, the energy loss caused by ligand vibration may decrease the emission intensity.

In contrast to EuIII and TbIII complex of similar ligand with 2,3-dimethoxy benzene as backbone and picolylsalicylamide as terminal group reported previously [6(i)], the lifetime of EuIII and TbIII complex are longer, for the triplet energy level of the antenna only changed slightly, which excludes the possibility that the increasing of luminescence is due to a change of the nature of the antenna

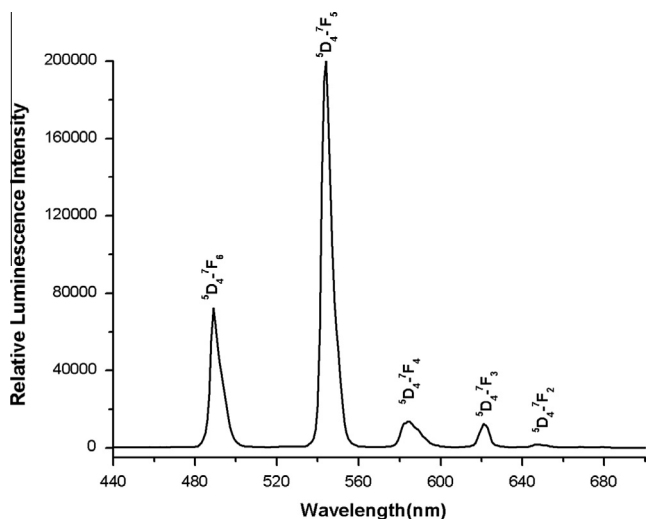


Fig. 6. Room-temperature emission spectra for terbium complex of ligand L ($\lambda_{\text{ex}} = 320\text{ nm}$) in the solid state.

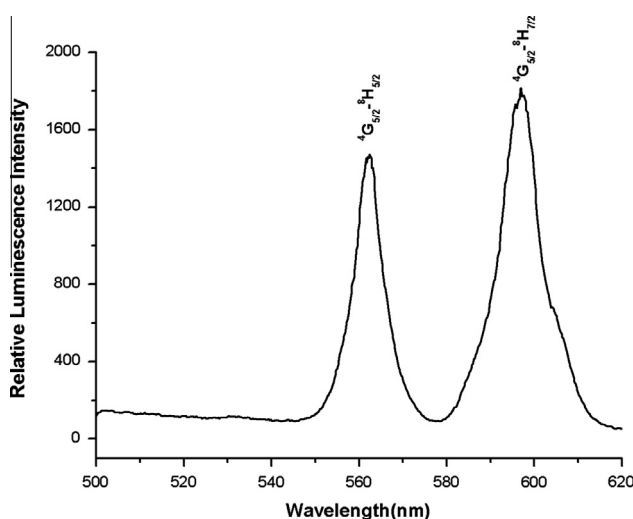


Fig. 8. Room-temperature emission spectra for samarium complex of ligand L ($\lambda_{\text{ex}} = 320\text{ nm}$) in the solid state.

triplet state. It is well-known that the presence of OH oscillators in the lanthanide first coordination sphere provides an efficient non-radiative path [21], so we can suggest that the observed increase in the lifetime of the 5D_4 level and the 5D_0 level is mainly related to an decrease in non-radiative transitions due to the decrease in the number of OH oscillators in the TbIII or EuIII first coordination shell of ligand with 2,3-dimethoxy benzene as backbone and picolylsalicylamide as terminal group, which is in perfect agreement with the proposed structural results.

4. Conclusions

We presented here a new semirigid bridging exobidentate ligands with terminal thenylsalicylamide groups, which resulted in the formation of 1D annular lanthanide coordination polymers with interesting supramolecular structures. It is interesting to note that the two salicylamide arms of L are somewhat flexible and rotational around the 1,4-dimethoxybenzene to provide LnIII a distorted biccapped square antiprismatic coordination geometry. In addition, the two-dimensional puckered supramolecular architectures formed by the weak C–H...O hydrogen bonds as well as π – π stacking interaction between the chains have a cooperative effect and participate in the stabilization of the architectures. Luminescence studies demonstrated that the semirigid bridging exobidentate ligands exhibits a good antenna effect with respect to the TbIII ion than that of EuIII. It is worth noting that the change of backbone groups is also a decisive factor in determining the coordination environments of the metal centers as well as luminescence properties. The results demonstrated herein serve to illustrate the potential of salicylamide ligands both with regard to constructing interesting supramolecular structures and for purposes of incorporating predictable physical properties.

Acknowledgements

This work was supported by the National Natural Science Foundation of China (Grants 21161011) and Gansu Natural Science Foundation of China (Grants 1212RJZA038).

Appendix A. Supplementary material

CCDC 929395–929398 contain the supplementary crystallographic data for this paper. These data can be obtained free of charge from The Cambridge Crystallographic Data Centre via http://www.ccdc.cam.ac.uk/data_request/cif. Supplementary data associated with this article can be found, in the online version, at <http://dx.doi.org/10.1016/j.ica.2013.08.014>.

References

- [1] a) J. Kido, Y. Okamoto, *Chem. Rev.* 102 (2002) 2357; b) M.A. Katkova, A.G. Vitukhnovsky, M.N. Bochkarev, *Russ. Chem. Rev.* 74 (2005) 1089; c) R.C. Evans, P. Douglas, C.J. Winscom, *Coord. Chem. Rev.* 250 (2006) 2093; d) A. de Bettencourt-Dias, *Dalton Trans.* (2007) 2229; e) J.-C.G. Bünzli, C. Piguet, *Chem. Soc. Rev.* 34 (2005) 1048; f) K. Binnemans, *Chem. Rev.* 109 (2009) 4283; g) S.V. Eliseeva, J.-C.G. Bünzli, *Chem. Soc. Rev.* 39 (2010) 189; h) J.-C.G. Bünzli, *Chem. Rev.* 110 (2010) 2729; i) K. Kuriki, Y. Koike, Y. Okamoto, *Chem. Rev.* 102 (2002) 2347.
- [2] (a) N. Sabbatini, M. Guardigli, J.-M. Lehn, *Coord. Chem. Rev.* 123 (1993) 201; (b) C. Piguet, J.-C.G. Bünzli, G. Bernardinelli, G. Hopfgartner, S. Petoud, O. Schaad, *J. Am. Chem. Soc.* 118 (1996) 6681.
- [3] (a) C.Y. Su, Y.P. Cai, C.L. Chen, B.S. Kang, *Inorg. Chem.* 40 (2001) 2210; (b) P. Ayyappan, O.R. Evans, W.B. Lin, *Inorg. Chem.* 40 (2001) 3328; (c) J. Fan, H.F. Zhu, T. Okamura, W.Y. Sun, W.X. Tang, N. Ueyama, *Inorg. Chem.* 42 (2003) 158; (d) Y. Cui, H.L. Ngo, W.B. Lin, *Inorg. Chem.* 41 (2002) 5940; (e) B.L. Chen, S.Q. Ma, F. Zapata, F.R. Fronczek, E.B. Lobkovsky, H.C. Zhou, *Inorg. Chem.* 46 (2007) 1233.
- [4] (a) X.H. Bu, W. Weng, W. Chen, R.H. Zhang, *Inorg. Chem.* 41 (2002) 413; (b) X.H. Bu, W. Weng, M. Du, W. Chen, J.R. Li, R.H. Zhang, L.J. Zhao, *Inorg. Chem.* 41 (2002) 1007; (c) J.R. Li, X.H. Bu, R.H. Zhang, C.Y. Duan, K.M.C. Wong, V.W.W. Yam, *New J. Chem.* 28 (2004) 261; (d) J.R. Li, X.H. Bu, R.H. Zhang, *Inorg. Chem.* 43 (2004) 237; (e) S.J. Dalgarno, M.J. Hardie, J.L. Atwood, C.L. Raston, *Inorg. Chem.* 43 (2004) 6351.
- [5] (a) X.D. Guo, G.S. Zhu, Q.R. Fang, M. Xue, G. Tian, J.Y. Sun, X.T. Li, S.L. Qiu, *Inorg. Chem.* 44 (2005) 3850; (b) C. Daiguebonne, N. Kerbellec, K. Bernot, Y. Gérault, A. Deluzet, O. Guillou, *Inorg. Chem.* 45 (2006) 5399; (c) C. Qin, X.L. Wang, E.B. Wang, Z.M. Su, *Inorg. Chem.* 44 (2005) 7122; (d) Z.H. Zhang, T. Okamura, Y. Hasegawa, H. Kawaguchi, L.Y. Kong, W.Y. Sun, N. Ueyama, *Inorg. Chem.* 44 (2005) 6219; (e) C. Marchal, Y. Filinchuk, D. Imbert, J.C.G. Bünzli, M. Mazzanti, *Inorg. Chem.* 46 (2007) 6242.
- [6] (a) Y. Tang, J. Zhang, W.-S. Liu, M.-Y. Tan, K.-B. Yu, *Polyhedron* 24 (2005) 1160; (b) X.-Q. Song, W.-S. Liu, W. Dou, Y.-W. Wang, J.-R. Zheng, Z.-P. Zang, *Eur. J. Inorg. Chem.* 11 (2008) 1901; (c) X.-Q. Song, X.-G. Weng, W.-S. Liu, D.-Q. Wang, *J. Solid State Chem.* 183 (2010) 1; (f) Q. Wang, X. Yan, H. Zhang, W. Liu, Y. Tang, M. Tan, *J. Solid State Chem.* 184 (2011) 64; (g) X.-Q. Song, W.K. Dong, Y.-J. Zhang, W.-S. Liu, *Luminescence* 25 (2010) 328; (h) X.-Q. Song, Q.-F. Zheng, L. Wang, W.-S. Liu, *Luminescence* 27 (2012) 459; (i) X.-Q. Song, L. Wang, Q.-F. Zheng, W.-S. Liu, *Inorg. Chim. Acta* 391 (2012) 171; (j) X.-Q. Song, L. Wang, M.-M. Zhao, G.-Q. Cheng, X.-R. Wang, Y.-P. Qiao, *Inorg. Chim. Acta* 402 (2013) 156; (k) X.-Q. Song, D.-Y. Xing, Y.-K. Lei, M.-M. Zhao, G.-Q. Cheng, X.-R. Wang, Y.-P. Qiao, *Inorg. Chim. Acta* 404 (2013) 113; (l) X.Y. Zhou, Y.L. Guo, Z.-H. Shi, X.-Q. Song, X.L. Tang, X. Hu, Z.T. Zhu, P.X. Li, *W.S. Liu, Dalton Trans.* 47 (2012) 1765.
- [7] (a) X.-Q. Song, X.-Y. Zhou, W.-S. Liu, W. Dou, J.-X. Ma, X.-L.G. Tang, J.-R. Zheng, *Inorg. Chem.* 24 (2008) 11501; (b) X.-Q. Song, W.-S. Liu, W. Dou, J.-R. Zheng, X.-L. Tang, H.-R. Zhang, D.-Q. Wang, *Dalton Trans.* 24 (2008) 3582; (c) X.-Y. Zhou, Y.-L. Guo, Z.-H. Shi, X.-Q. Song, X.-L. Tang, X. Hu, Z.-T. Zhu, P.-X. Li, W.-S. Liu, *Dalton Trans.* 41 (2012) 1765.
- [8] K. Nakagawa, K. Amita, H. Mizuno, Y. Inoue, T. Hakushi, *Bull. Chem. Soc. Jpn.* 60 (1987) 2037.
- [9] F. Gutierrez, C. Tedeschi, L. Maron, J.-P. Daudey, R. Poteau, J. Azema, P. Tisnès, C. Picard, *Dalton Trans.* 9 (2004) 1334.
- [10] (a) C. De Mello, H.F. Wittmann, R.H. Friend, *Adv. Mater.* 9 (1997) 230; (b) L.-O. Palsson, A.P. Monkman, *Adv. Mater.* 14 (2002) 757.
- [11] Z. Jiri, P. Magdalena, H. Petr, T. Milos, *Synthesis* 110 (1994) 1132.
- [12] G.M. Sheldrick, SHELXL-97, Program for Crystal Structure Solution and Refinement, University of Göttingen, Göttingen, Germany, 1997.
- [13] K. Nakamoto, *Infrared and Raman Spectra of Inorganic and Coordination Compounds*, Wiley, New York, 1978, p. 227.
- [14] A.J. Zhang, Y. Wen Wang, W. Dou, M. Dong, Y.L. Zhang, Y. Tang, W.S. Liu, Y. Peng, *Dalton Trans.* 40 (2011) 2844.
- [15] G.A. Jeffrey, H. Maluszynska, J. Mitra, *Int. J. Biol. Macromol.* 7 (1985) 336.
- [16] M. Albin, R.R. Whittle, W.D. Horrocks Jr., *Inorg. Chem.* 24 (1985) 4591.
- [17] A.F. Kirby, D. Foster, F.S. Richardson, *Chem. Phys. Lett.* 95 (1983) 507.
- [18] (a) I. Klink, L. Grave, D.N. Reinhoudt, F.C.J.M. van Veggel, M.H.V. Werts, F.A.J. Geurts, J.W. Hofstraat, *J. Phys. Chem. A* 104 (2000) 5457; (b) J. Xia, B. Zhao, H.-S. Wang, W. Shi, Y. Ma, H.-B. Song, P. Cheng, D.-Z. Liao, S.-P. Yan, *Inorg. Chem.* 46 (2007) 3450.
- [19] M. Latva, H. Takalo, V.M. Mikkala, C. Matachescu, J.C. Rodriguez-Ubis, J. Kanakare, *J. Lumin.* 75 (1997) 149.
- [20] S.W. Magennis, S. Parsons, Z. Pikramenou, *Chem. Eur. J.* 8 (2002) 5761.
- [21] W.D. Horrocks, D.R. Sudnick, *J. Am. Chem. Soc.* 101 (1979) 334.